



# Sulfurization of carbon surface for vapor phase mercury removal – I: Effect of temperature and sulfurization protocol

Wenguo Feng <sup>a</sup>, Eric Borguet <sup>b</sup>, Radisav D. Vidic <sup>a,\*</sup>

<sup>a</sup> Department of Civil and Environmental Engineering, University of Pittsburgh, 949 Benedum Hall, Pittsburgh, PA 15261, United States

<sup>b</sup> Department of Chemistry, Temple University, 1901 N., 13th Street, Philadelphia, PA 19122, United States

Received 25 October 2005; accepted 18 May 2006

Available online 11 July 2006

---

## Abstract

The uptake of hydrogen sulfide by carbon materials (ACFs and BPL) under dry and anoxic conditions was tested using a fixed bed reactor system to determine the effects of sorbent properties, temperature (200–800 °C) and sulfurization protocols on the sulfur content, sulfur stability, sulfur distribution, and to elucidate possible reaction mechanisms for the formation of sulfur species. Sorbents with higher surface areas showed higher uptake capacity, indicating that active sites for sulfur bonding are formed during the formation of the pore structure. The sulfur content and stability generally increased with the increase in temperature due to a shift in the reaction mechanism. The sulfurization process is associated with the decomposition of surface functionalities, which creates active sites for sulfur bonding. The presence of H<sub>2</sub>S during the cooling process increased the sulfur content by increasing the presence of less stable sulfur forms. Sulfurized sorbents produced at high temperatures have pore structure similar to that of the virgin carbons.

© 2006 Elsevier Ltd. All rights reserved.

*Keywords:* Activated carbon; Carbon fibers; Impregnation; Temperature programmed desorption; Surface properties

---

## 1. Introduction

Hydrogen sulfide is an odorous pollutant and it is commonly regarded as toxic [1–3]. In addition to its health effects, hydrogen sulfide is a corrosive gas, exerting adverse effects in many industrial processes. Many of those processes are characterized by hydrogen sulfide streams at relatively low temperatures, e.g., the tail gas from the Claus process and natural gas sweetening. However, in some processes, such as the Integrated Gasification Combined Cycle (IGCC) process [4], and the coal gas cleaning process [5], removal of hydrogen sulfide must be accomplished at elevated temperatures (300–800 °C) and pressures (300–1000 psi).

Carbon-based sorbents have been evaluated for the removal of hydrogen sulfide due to the need to control odorous gases generated in sewer systems and wastewater treatment plants at ambient conditions [6–8]. Those studies

concluded that the surface area and pore volume are not the only factors contributing to H<sub>2</sub>S adsorption, and that surface chemistry played a significant role in the uptake of H<sub>2</sub>S. Mikhailovsky and Zaitsev [9] showed that H<sub>2</sub>S adsorption from an inert atmosphere on activated carbons resulted in the formation of elemental sulfur, thereby suggesting that the adsorption of hydrogen sulfide on carbon surface may be dissociative.

The term “sulfurization” is used here to describe the process of sulfur incorporation into the carbon matrix or on the carbon surface at high temperatures. Sulfurization of carbon surfaces has been studied over the past few decades and many mechanisms were proposed. According to Puri [10], formation of C–S complex with sulfur containing gases, such as H<sub>2</sub>S, CS<sub>2</sub>, SO<sub>2</sub>, and sulfur vapor, was observed at 100–1000°C. Blayden and Patrick [11] studied the formation and behavior of sulfur containing carbons by heating the polymeric carbon in the presence of elemental sulfur. They proposed that the unpaired spin centers and hydrogen content might play important roles in the

---

\* Corresponding author. Tel.: +1 412 624 1307; fax: +1 412 624 0135.  
E-mail address: [vidic@pitt.edu](mailto:vidic@pitt.edu) (R.D. Vidic).

sulfurization of the carbon surface. The bonding of C–S complexes was postulated to be akin to that of thioethers or disulfides.

Significant amount of sulfur can be fixed by the carbon materials through sulfurization at various temperatures. Kor [12,13] reported that a significant amount of sulfur was incorporated in carbon or coal from a gas containing H<sub>2</sub>S. Valenzuela Calahorro et al. [14] reported that about 9.9 wt.% of sulfur was incorporated into the carbon surface by heating activated carbon in high concentrations of H<sub>2</sub>S. All carbon–sulfur complexes formed through these reactions were found to be very stable [10]. Hydrogen sulfide and carbon disulfide were found in the effluent gas when the resulting impregnated sorbent was heated to 500 °C and the amount of emitted gases increased with the increase in temperature. However, an appreciable amount of sulfur was retained by the carbon even after heating the samples to 1200 °C. The sulfur could only be completely removed by heating the product in hydrogen at 900 °C [10].

It was postulated that H<sub>2</sub>S interacts with quinonic and phenolic (or hydroxyl) groups to produce thioquinone and thiophenol groups [10]. The rest of the loosely bonded sulfur was added to the unsaturated sites that are not very reactive. As a result, sulfide and hydrosulfide groups could also be produced. Puri and Hazra [15] observed that the amount of sulfur fixed on the carbon surface correlates well with the oxygen content present as “CO-Complex” (the oxygen containing complex released as CO upon heat treatment). The authors believe that oxygen and hydrogen content, extent of surface unsaturation (vacancies on the surface), and pore structure were more important parameters than surface area.

Sugawara et al. [16] studied the effect of hydrogen sulfide on the behavior of organic sulfur in coal and char during heat treatment up to 1073 K. Sulfur forms in the samples were determined using Sulfur K-edge X-ray adsorption near-edge structure spectroscopy. They concluded that a considerable amount of hydrogen sulfide was absorbed during heat treatment, forming organic sulfur forms, such as thiophenes and sulfides. These forms of sulfur tend to concentrate as the gasification proceeds. Ozaki et al. [17] reported the decomposition of H<sub>2</sub>S on iron impregnated thermally stable turbostratic carbons, which were derived from furan resin. The surface iron species were believed to be responsible for the decomposition of H<sub>2</sub>S around 350 °C, while the decomposition of H<sub>2</sub>S above 600 °C was attributed to Lewis acidic site. Cal et al. [4,18] studied the effects of surface modifications on the removal of H<sub>2</sub>S from a simulated coal gas by activated carbon. Both HNO<sub>3</sub> oxidation and Zn impregnation improved H<sub>2</sub>S adsorption capacity. The following three mechanisms explain part of the chemisorption of hydrogen sulfide on activated carbon surface [4,18]:

- Addition to carbon active sites:  $C + H_2S = C-S + H_2$
- Substitution of oxygen:  $C-O + H_2S = C-S + H_2O$
- Reaction with metals:  $C-M + H_2S = C-M-S + H_2$

In addition to carbon surfaces, hydrocarbons can also be sulfurized under different conditions. There are several reports about sulfurization of organic matter by sulfides in aqueous phase at low temperature (around 50 °C) [19,20]. These studies revealed the formation of sulfur-rich compounds. Van Dongen et al. [19,21] proposed that the reaction most likely starts with sulfurization of the carbonyl functionality. It was also showed that sulfur can be incorporated onto the surface of polymers, thereby resulting in significant increase in the surface sulfur content [22,23]. Thiophenes and polysulfides were believed to be the possible products. CH<sub>4</sub> and H<sub>2</sub>S were found to react in a plasma reactor to produce a thin film containing about 27% of sulfur [24,25]. The produced film was believed to have polymeric structure of (CS<sub>2</sub>)<sub>x</sub>. Besides hydrocarbons, many metals or metal oxide surfaces (such as Fe, Pd, and Ni) can be easily sulfurized [26,27]. These observations are helpful to understand the sulfurization of carbon surfaces.

Sulfurization of carbon surfaces is a complicated process in need of further investigation. In addition, sulfur impregnated carbon materials hold the promise for controlling mercury pollution. It was reported that sulfur impregnated activated carbons can effectively and permanently remove mercury from flue gas streams [28–30]. Sulfurization by hydrogen sulfide may be a possible way of producing effective mercury sorbents [31]. This part of the study was designed to further investigate sulfurization process in an effort to understand the parameters that affect sulfur content, stability, distribution, and sulfurization mechanism on the surface of activated carbon materials.

## 2. Experimental details

### 2.1. Carbon materials

Three activated carbon fibers (ACFs, American Kynol, Inc., Pleasantville, NY), namely, ACF-10, ACF-20, and ACF-25, were used in this study. ACFs were dried and ground into powder before loading into the reactor. Commercially available activated carbon, BPL (Calgon Carbon Corporation, Pittsburgh, PA) was sieved to 16 × 50 US mesh size for use in this study. The virgin ACFs have extremely low sulfur content (0.02 wt.%) while the virgin BPL carbon has initial sulfur content of 0.75 wt.%. The sources and chemical compositions of all sorbents are summarized in Table 1. Compared to BPL, ACFs have negligible ash content due to significantly lower impurities in the raw material. Major elements in both sorbents are carbon and oxygen with very limited amount of hydrogen and nitrogen. Previous studies indicated that the oxygen content of ACFs decreased with an increase in serial number [32–34]. Surface areas and pore structures of the sorbents used in this study are listed in Table 2. With the increase in ACF serial number, the surface area and pore volume increase because ACFs with higher serial number are produced with higher burn-off. The extended activation produces more

Table 1  
Sources and chemical compositions of BPL and ACFs

Carbon	Base material	Ash content (wt.%)	Elemental composition (wt.%)				
			O	C	H	N	S
BPL	Bituminous coal	6.6	5.40 <sup>a</sup>	–	–	–	0.75
ACF-10	Resin	0.01	8.11 <sup>b</sup>	91.4 <sup>b</sup>	0.33 <sup>b</sup>	0.16 <sup>b</sup>	0.02
ACF-20	Resin	0.01	–	–	–	–	0.02
ACF-25	Resin	0.01	4.50 <sup>b</sup>	95.2 <sup>b</sup>	0.06 <sup>b</sup>	0.24 <sup>b</sup>	0.02

<sup>a</sup> Zhu et al. [38].

<sup>b</sup> Mangun et al. [32,33]; similar data were also reported by Foster et al. [34].

Table 2  
Surface areas and pore structures of BPL and ACFs

Carbon material	BET surface area (m <sup>2</sup> /g)	Pore volume (cm <sup>3</sup> /g)	Micropore volume (cm <sup>3</sup> /g)	Percent of micropores (%)
BPL	1067	0.581	0.408	70
ACF-10	920	0.378	0.374	99
ACF-20	1453	0.691	0.666	96
ACF-25	1950	0.853	0.806	94

active sites, higher surface areas, and larger pore volume. Compared to BPL, ACFs have more uniform pore size distribution and almost all of the pores are in the micropore region.

## 2.2. H<sub>2</sub>S uptake test

A fixed bed reactor system was used for H<sub>2</sub>S uptake test. Desired influent H<sub>2</sub>S streams were generated by diluting 5% H<sub>2</sub>S in nitrogen (Praxair, certified) with nitrogen (Praxair, UHP). Mixed gas with a total flow rate of 150 ml/min was fed through a quartz reactor (38 cm long with 1 cm OD), which was positioned in the middle of a vertical tubular furnace (Lindberg Heavi-Duty, Watertown, WI). Five hundred milligrams of carbon sample was loaded in the reactor. After drying at 120 °C for 2 h and cooling to ambient temperature, sulfurization of carbon surfaces was car-

ried out using 10 °C/min heating rate to a stable temperature (400–800 °C) with exposure of the carbon surface to H<sub>2</sub>S at different stages. As shown in Fig. 1, the following samples were prepared at maximum stable temperature of 600 °C and H<sub>2</sub>S concentration of 3000 ppm: for 600C–S Only, H<sub>2</sub>S was fed to the reactor during stable temperature only; for 600C–H + S, H<sub>2</sub>S was fed to the reactor during heating and stable temperature; for 600C–H + S + C, H<sub>2</sub>S was fed to the reactor during heating, stable temperature, and cooling; for 600C–S + C, H<sub>2</sub>S was fed to the reactor during stable temperature and cooling; and for 600C only, H<sub>2</sub>S was fed to the reactor during the cooling process only. Using Quadrupole Mass Spectrometer (QMS 300, Stanford Research Systems, Sunnyvale, CA) to monitor the exit gas, it was determined that 6 h of exposure to H<sub>2</sub>S was sufficient to reach complete breakthrough of H<sub>2</sub>S under all conditions. Sulfur analysis

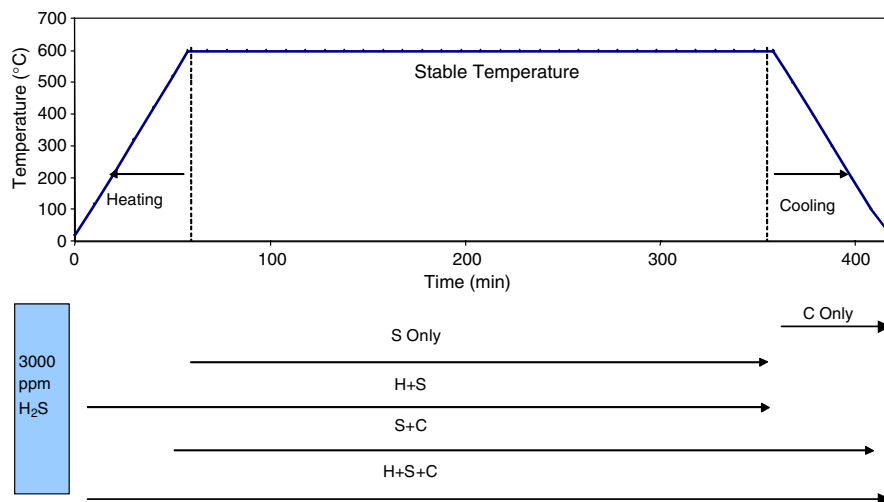


Fig. 1. Experimental protocols for the sulfurization process.

also confirmed that no increase in the sulfur content was observed even if the impregnation time was increased to 14 h. For all the runs, the stable temperature period lasted for 6 h.

### 2.3. Sorbent characterization

Sulfurized sorbents were subjected to different characterization methods. Sulfur content was measured using a sulfur analyzer (SC-132, Leco Sulfur Analyzer, St. Joseph, MI). The surface area and pore size distribution of virgin and impregnated ACFs were analyzed using nitrogen adsorption at 77 K in a Quantachrome Autosorb Automated Gas Sorption System (Quantachrome Corporation, Boynton Beach, FL). Thermogravimetric analysis (TGA) was conducted using a TGA7 (Perkin–Elmer, Norwalk, CT) where the sample was maintained at 120 °C for 2 h and then heated to 850 °C with a heating rate of 10 °C/min in a high purity nitrogen atmosphere. SEM (Scanning Electron Microscope) – EDAX (Energy Dispersive Analysis, X-ray) analysis was conducted using a Philips XL30 SEM equipped with an EDAX detector. EDAX detector was used to measure elemental composition of the ACF samples that were pasted as a thick layer onto a tape before insertion into the vacuum chamber.

### 2.4. Temperature programmed desorption and temperature programmed reaction

Temperature programmed desorption of virgin BPL carbon was conducted using 1 g of BPL carbon in a fixed bed reactor. Starting from room temperature, the temperature of the tubular furnace was raised to 900 °C at 10 °C/min in a 30 ml/min argon gas stream and effluent gas was monitored with the QMS300. AMUs of interest and the desorption temperatures were recorded continuously.

Temperature programmed reaction was conducted in a similar way with 1 g of BPL carbon. After a complete breakthrough from a sorbent bed maintained at room temperature and fed 30 ml/min of 12,000 ppm H<sub>2</sub>S stream generated by diluting 5% H<sub>2</sub>S in nitrogen with argon, the reactor was heated to 900 °C at 10 °C/min while continuing to feed the same flow and composition of the influent gas.

## 3. Results and discussion

### 3.1. Effect of carbon materials

Four carbon materials (i.e., three ACFs and BPL carbon) were tested for H<sub>2</sub>S uptake at 600 °C (600 C–S Only). The results in Fig. 2 clearly show that for all the carbon materials tested, the increased sulfur content (the ultimate sulfur content minus the sulfur content of the virgin carbons) showed good correlation with the surface area of virgin carbon material. Because BPL carbon is manufactured from coal, it can be expected to have a significant metal content on its surface [35]. Surprisingly, metal content on

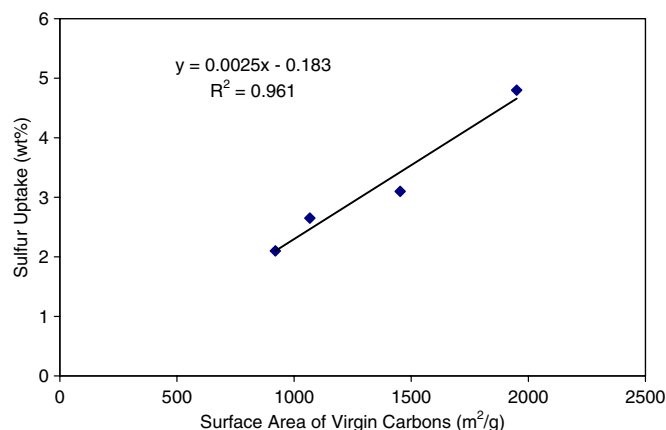


Fig. 2. Effect of sorbent surface area on the increased sulfur content after sulfurization.

BPL carbon did not result in higher hydrogen sulfide uptake, indicating that its metals are not effective sites for hydrogen sulfide uptake. As shown in Table 1, with the increase in ACF serial number, the oxygen content decreases. This suggests that the oxygen containing functionalities as a whole are not the major factor for H<sub>2</sub>S uptake either. These results support the hypothesis that the active sites for H<sub>2</sub>S uptake at high temperature are closely related to the pore structure, indicating that they are derived from the carbon structure itself. As discussed by Mangun et al. [33], the active sites on ACFs for SO<sub>2</sub> uptake are probably the defect sites, which can be created by oxidation and then degassing.

### 3.2. Effect of temperature

Fig. 3 shows the effect of temperature in the range of 400–800 °C on ultimate sulfur content of ACF-25 and BPL carbon with H<sub>2</sub>S fed to the reactor during the stable temperature only (S Only). Sulfur loading on these carbonaceous sorbents increased with an increase in temperature. These samples have much higher sulfur content than

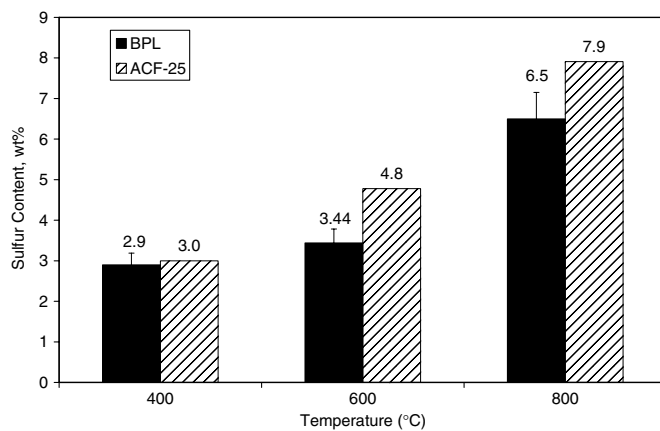


Fig. 3. Effect of temperature on sulfurization of ACF25 and BPL in the presence of H<sub>2</sub>S during stable temperatures only (S only).

those produced at low temperatures [36]. Such behavior is reasonable since the higher temperature can provide more energy to facilitate greater interaction between  $\text{H}_2\text{S}$  and carbon surface and promote formation of more active sites for  $\text{H}_2\text{S}$  uptake.

Fig. 4 depicts temperature programmed desorption (TPD) profile of virgin BPL. The major decomposition products of the surface functional groups are  $\text{CO}_2$  at lower temperatures and  $\text{CO}$  at higher temperatures. The maximum release of the two gases occurred at 370 °C (643 K) and 790 °C (1063 K), respectively. Similar results were also reported by Li et al. [37]. The increase in temperature leads to the decomposition of more surface functionalities, thereby creating more active sites for sulfur bonding, and leading to higher sulfur content at higher temperatures. These observations agree with the mechanism proposed by Mangun et al. [33] for  $\text{SO}_2$  uptake. Since the temperature ranges for the decomposing of the surface functionalities are different, the reactivity of these active sites towards  $\text{H}_2\text{S}$  may not be the same.

The temperature programmed reaction results shown in Fig. 5 can provide further insight into the reaction mechanism. Complete breakthrough of  $\text{H}_2\text{S}$  at room temperature occurred after about 25 min (Fig. 5(a)). Once the reactor heating commenced, two  $\text{H}_2\text{S}$  peaks representing the desorption of weakly and strongly adsorbed  $\text{H}_2\text{S}$  were observed at 50 and 450 °C, respectively (Fig. 5(a)). Similar results were reported in previous studies of  $\text{H}_2\text{S}$  adsorption onto carbon surfaces at low temperatures [36]. At reactor temperatures between 150 °C and 600 °C, there is no significant decrease in  $\text{H}_2\text{S}$  concentration and no other sulfur containing gas species were observed in the gas stream (Fig. 5(b)). This indicates adsorption of  $\text{H}_2\text{S}$  in this temperature range could be attributed to addition to unsaturated active sites created by the decomposition of  $\text{CO}_2$  yielding functionalities or addition to “CO-Complex” as proposed by Puri and Hazra [15]. Above 600 °C, the concentration of  $\text{H}_2\text{S}$  started to decrease dramatically. At the same time, the formation of  $\text{H}_2$  was observed (data not shown), indicating the decomposition of  $\text{H}_2\text{S}$  to  $\text{H}_2$  and S that is cata-

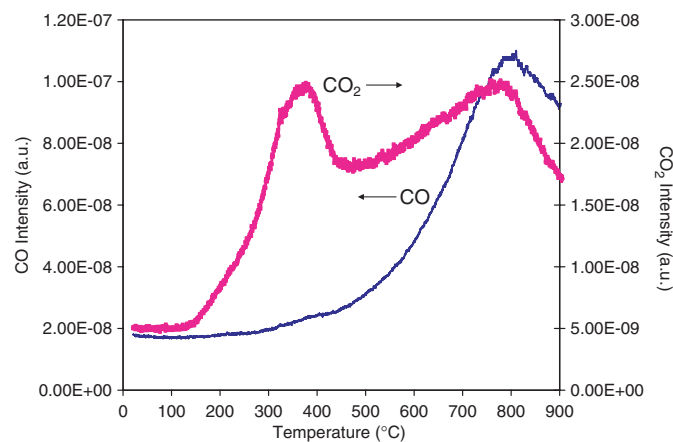


Fig. 4.  $\text{CO}_2$  and  $\text{CO}$  evolution during temperature programmed desorption from BPL carbon in argon at 10 °C/min.

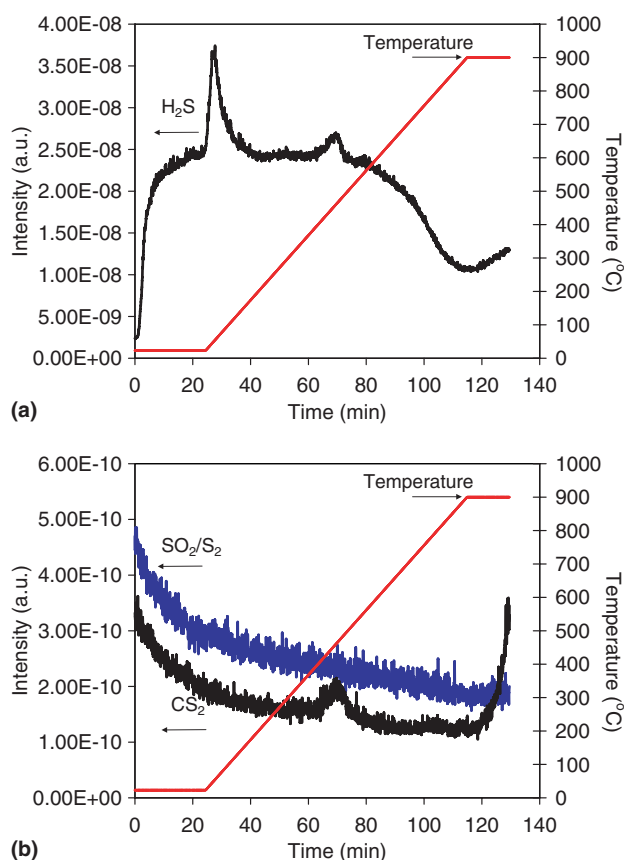


Fig. 5. Temperature programmed reaction between  $\text{H}_2\text{S}$  and BPL surface. (a)  $\text{H}_2\text{S}$  profile and (b) other sulfurous compounds in the effluent.

lyzed by the carbon surface (no  $\text{H}_2$  was observed during sample heating in the absence of  $\text{H}_2\text{S}$ ). This hypothesis is supported by the observation of yellow elemental sulfur at the exit of the reactor. Above 800 °C, another species,  $\text{CS}_2$ , started to evolve (Fig. 5(b)). This suggests the direct chemical reaction between carbon and  $\text{H}_2\text{S}$ , and possible incorporation of sulfur into the graphite structure.

EDAX was used to determine elemental composition of the surface of ACF-25. The S, O, and C contents on the surface were determined after sulfurization at different temperatures and the surface sulfur content is compared with that obtained from the bulk sulfur analysis by Leco Sulfur Analyzer in Table 3. The increase in temperature led to a decrease in oxygen/carbon content and increase in the sulfur content. Such behavior suggest that uptake of  $\text{H}_2\text{S}$  is associated with the decomposition of carbon surface

Table 3  
Sulfur content (S Only) in the bulk (sulfur analysis) and on the surface (EDAX)

Sample	Bulk sulfur content (wt.%)	Surface content (wt.%)		
		S	O	C
ACF25-Virgin	0.2	0.2	4.38	95.41
ACF25-400C-S only	3.0	6.04	2.13	91.83
ACF25-600C-S only	4.8	6.95	1.61	91.44
ACF25-800C-S only	7.9	11.52	1.31	87.17



functionalities and loss of active carbon atoms. The loss of active carbon atoms, forming volatile carbon disulfide, was observed at temperatures above 500 °C (data not shown). Sulfur content on the surface is higher than that in the bulk because the gas-solid reaction between H<sub>2</sub>S and carbon occurs mainly on the external surface.

Fig. 6 shows the effect of temperature on ultimate sulfur content of BPL carbon exposed to H<sub>2</sub>S throughout the entire process and associated TGA results. Fig. 6 shows that the sulfur content in general increases with the increase in temperature, which can be explained by the creation of more active sites for sulfur binding. The peak in sulfur content around 300 °C may be associated with the peak in decomposition of functionalities yielding CO<sub>2</sub>. This result seems to support the hypothesis of Puri and Hazra [15] that “CO-Complex” enhances H<sub>2</sub>S adsorption.

TGA test results in Fig. 6 indicate that the dominant weight loss occurred in the temperature range from 300 °C to 500 °C. It is also evident that activated carbons impregnated with sulfur at temperatures below 400 °C lost most of the deposited sulfur during the TGA test. On the other hand, the sulfur content of carbons impregnated at 600 °C and 800 °C was much higher than the total weight loss, which means that sulfur was more strongly bonded to the carbon surface, which may be due to the formation of strongly bonded sulfur forms (e.g. organic sulfur). Formation of very stable sulfur species at 800 °C were also reported by Sugawara et al. [16].

### 3.3. Effect of sulfurization protocol

It can be seen from Fig. 7 that the presence of H<sub>2</sub>S during the heating and cooling process can increase the total sulfur content of BPL at 600 °C. Similar behavior was observed at other impregnation temperatures (data not shown). The difference in the ultimate sulfur content of samples produced at different temperatures is clearly due to the presence of H<sub>2</sub>S during the heating and cooling process. For BPL-600 C–C only, the sulfur content is lower than the other samples. However, considering the short

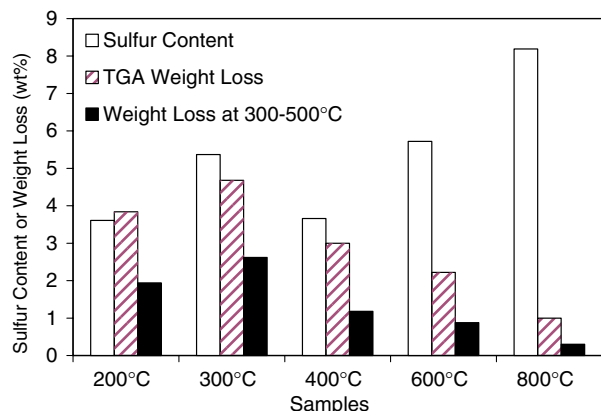


Fig. 6. Sulfur content and TGA results of BPL sorbents produced at different temperatures (H + S + C).

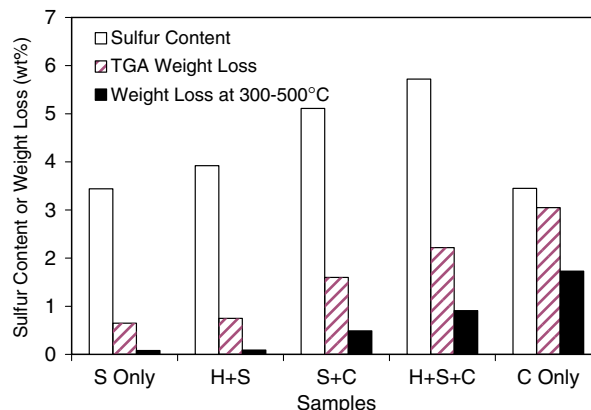


Fig. 7. Sulfur Content and TGA results of BPL sorbent produced by different sulfurization protocols at 600 °C.

duration of the cooling process (about 60 min), the uptake of sulfur is significant. Two factors may contribute to the increased uptake of sulfur during the cooling process. Firstly, the hydrogen sulfide molecules could not escape from the carbon surface once they are attached to the active sites (created at higher temperatures) because of the decreasing temperature; secondly, the carbon structure itself experiences an annealing process, which may also help to capture more sulfur species due the structural changes.

TGA test depicted in Fig. 7 showed that the three samples (600C–C Only, 600C–H + S + C and 600C–S + C) with the presence of H<sub>2</sub>S during the cooling process have much higher weight loss than 600C–H + S only and that 600C–H + S + C has the highest weight loss. Weight loss mainly occurred at the temperature range of 300–500 °C. Again this indicates that the sulfur added during the cooling process was not very strongly bonded to the carbon surface, but most probably was trapped as free elemental sulfur.

### 3.4. Sulfur distribution

Pore size distribution for BPL before and after hydrogen sulfide uptake shown in Fig. 8 suggests a slight change in

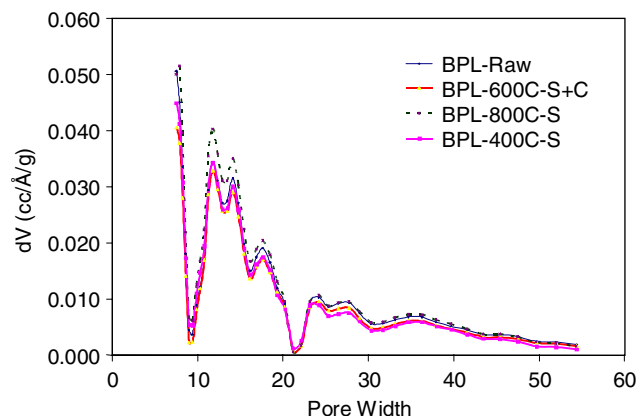


Fig. 8. Pore size distributions of BPL before and after H<sub>2</sub>S uptake at high temperatures.

pore volume in the 10–20 Å range after sulfurization. The presence of H<sub>2</sub>S during the cooling process further decreased the pore volume at smaller pore size range. However, the change in pore size distribution after hydrogen sulfide uptake is not significant. Such observation leads to the conclusion that the sulfurous compounds produced are extremely well distributed on the surface of the sorbent. Furthermore, it is more likely that the organic sulfur or chemically fixed elemental sulfur is the dominant sulfur form since the free elemental sulfur would tend to agglomerate into isolated islands on the carbon surface and significantly alter the pore size distribution of the sorbent.

#### 4. Conclusions

The uptake of hydrogen sulfide at 600 °C correlates well with the surface area of the carbon materials, indicating the formation of active sites during the formation of the pore structure. Sulfurization at higher temperatures resulted in higher sulfur content and more stable sulfur species. At temperatures below 600 °C, sulfurization is likely occurring through the addition of H<sub>2</sub>S onto active sites enhanced by decomposition of CO<sub>2</sub> yielding oxygen containing functionalities, while at higher temperatures direct reaction between H<sub>2</sub>S and the carbon probably occurred. The presence of H<sub>2</sub>S during the cooling process obviously increased the ultimate sulfur content, especially with relatively unstable species. Sulfurized sorbents produced at temperatures higher than 400 °C maintained pore structures similar to that of the virgin carbon. These results emphasize the influence of temperature on predominant sulfur forms created through thermal decomposition of H<sub>2</sub>S.

#### Acknowledgement

This study is supported by the NSF Grant No. BES-0202015. The authors would like to thank Dr. Seokjoon Kwon at Connecticut Agriculture Experimental Station for his help with pore size distribution analysis.

#### References

- [1] Brenneman KA, James RA, Gross EA, Dorman DC. Olfactory neuron loss in adult male CD rats following subchronic inhalation exposure to hydrogen sulfide. *Toxicol Pathol* 2000;28(2):326–33.
- [2] Guidotti TL. Occupational exposure to hydrogen–sulfide in the sour gas-industry – some unresolved issues. *Int Arch Occ Environ Health* 1994;66(3):153–60.
- [3] Dorman DC, Moulin FJM, McManus BE, Mahle KC, James RA, Struve MF, et al. Cytochrome oxidase inhibition induced by acute hydrogen sulfide inhalation: Correlation with tissue sulfide concentrations in the rat brain, liver, lung, and nasal epithelium. *Toxicol Sci* 2002;65(1):18–25.
- [4] Cal MP, Strickler BW, Lizzio AA. High temperature hydrogen sulfide adsorption on activated carbon I. Effects of gas composition and metal addition. *Carbon* 2000;38(13):1757–65.
- [5] Farrauto R, Hwang S, Shore L, Ruettinger W, Lampert J, Giroux T, et al. New material needs for hydrocarbon fuel processing: Generating hydrogen for the PEM fuel cell. *Annual Rev Mater Res* 2003;33:1–27.
- [6] Bandosz TJ. On the adsorption/oxidation of hydrogen sulfide on activated carbons at ambient temperatures. *J Colloid Interface Sci* 2002;246(1):1–20.
- [7] Bandosz TJ. Effect of pore structure and surface chemistry of virgin activated carbons on removal of hydrogen sulfide. *Carbon* 1999;37(3):483–91.
- [8] Bandosz T, Askew S, Kelly WR, Bagreev A, Adib F, Turk A, et al. Biofiltering action on hydrogen sulfide by unmodified activated carbon in sewage treatment plants. *Water Sci Technol* 2000;42(1–2):399–401.
- [9] Mikhlovsky SV, Zaitsev YP. Catalytic properties of activated carbons. I. Gas-phase oxidation of hydrogen sulfide. *Carbon* 1997;35(9):1367–74.
- [10] Puri BR. Surface complexes on carbon. In: Walker PL, editor. *Chemistry and physics of carbon*, vol. 6. New York; Marcel Dekker (New York, USA): American Carbon Society; 1970.
- [11] Blyden HE, Patrick JW. Solid complexes of carbon and sulfur- I. Sulfurized polymer carbons. *Carbon* 1967;5:533–44.
- [12] Kor GJW. Desulfurization and sulfidation of coal and coal char.1. desulfurization of coal and coal char at various temperatures and pressures. In: ACS 173rd Natl meet, symposium on desulfurization of coal and coal char. New Orleans LA USA, American Chemical Society, Division of Fuel Chemistry, 1977;22(2): 1–27.
- [13] Kor GJW. Desulfurization and Sulfidation of Coal and Coal Char.2. Sulfidation of Coal Char and Synthetic Chars. In: ACS 173rd Natl meet, symposium on desulfurization of coal and coal char. New Orleans LA USA, American Chemical Society, Division of Fuel Chemistry, 1977;22(2):1–27.
- [14] Valenzuela Calahorra C, Macias Garcia A, Bernalte Garcia A, Gomez Serrano V. Study of sulfur introduction in activated carbon. *Carbon* 1990;28:321–35.
- [15] Puri BR, Hazra RS. Carbon–sulfur surface complex on charcoal. *Carbon* 1971;9:123–34.
- [16] Sugawara K, Enda Y, Kato T, Sugawara T, Shirai M. Effect of hydrogen sulfide on organic sulfur behavior in coal and char during heat treatments. *Energy Fuels* 2003;17(1):204–9.
- [17] Ozaki J, Yoshimoto Y, Oya A, Takarada T, Kuznetsov VV, Ismagilov ZR, et al. H<sub>2</sub>S decomposition activity of TS carbon derived from furan resin. *Carbon* 2001;39(10):1611–2.
- [18] Cal MP, Strickler BW, Lizzio AA, Gangwal SK. High temperature hydrogen sulfide adsorption on activated carbon II. Effects of gas temperature, gas pressure and sorbent regeneration. *Carbon* 2000;38(13):1767–74.
- [19] van Dongen BE, Schouten S, Baas M, Geenevasen JAJ, Damste JSS. An experimental study of the low-temperature sulfurization of carbohydrates. *Org Geochem* 2003;34(8):1129–44.
- [20] Kok MD, Schouten S, Damste JSS. Formation of insoluble, nonhydrolyzable, sulfur-rich macromolecules via incorporation of inorganic sulfur species into algal carbohydrates. 2000;64(15):2689–99.
- [21] van Dongen BE, Schouten S, Damste JSS. Sulfurization of carbohydrates results in a sulfur-rich, unresolved complex mixture in kerogen pyrolysates. *Energy Fuels* 2003;17(4):1109–18.
- [22] Trofimov BA, Skotheim TA, Mal'kina AG, Sokolyanskaya LV, Myachina GF, Korzhova SA, et al. Sulfurization of polymers 3. Paramagnetic and redox properties of sulfurized polyethylene. *Russian Chem Bull* 2000;49(5):870–3.
- [23] Trofimov BA, Skotheim TA, Mal'kina AG, Sokolyanskaya LV, Myachina GF, Korzhova SA, et al. Sulfurization of polymers 2. Polythienothiophene and related structures from polyethylene and elemental sulfur. *Russian Chem Bull* 2000;49(5):863–9.
- [24] Filik J, Lane IM, May PW, Pearce SRJ, Hallam KR. Incorporation of sulfur into hydrogenated amorphous carbon films. *Diamond Related Mater* 2004;13:1377–84.
- [25] Kim MC, Cho SH, Lee SH, Kim Y, Boo JH. Characterization of polymer-like thin films deposited on silicon and glass substrates using PECVD method. *Thin solid films* 2004;30:592–8.
- [26] Saleh JM. Interaction of sulfur compounds with palladium. *Trans Faraday Soc* 1970;66(1):242–50.

- [27] Bak Y-C, Choi J-H. High temperature sulphidation behavior of Fe-based and Ni-based alloys. *Hwahak Konghak* 2003;41(2):243–8.
- [28] Liu W. Development of novel adsorbents for the control of vapor-phase mercury emissions. Pittsburgh PA USA, University of Pittsburgh, Ph.D. Thesis, 1999.
- [29] Liu W, Vidic RD, Brown TD. Optimization of sulfur impregnation protocol for fixed bed application of activated carbon-based sorbents for gas-phase mercury removal. *Environ Sci Technol* 1998;32(4):531–8.
- [30] Liu W, Vidic RD, Brown TD. Optimization of high temperature sulfur impregnation on activated carbon for permanent sequestration of elemental mercury vapors. *Environ Sci Technol* 2000;34(3):483–8.
- [31] Kwon S, Vidic RD. Evaluation of two sulfur impregnation methods on activated carbon and bentonite for the production of elemental mercury sorbents. *Environ Eng Sci* 2000;17(6):303–13.
- [32] Mangun CL, Benak KR, Economy J, Foster KL. Surface chemistry, pore sizes and adsorption properties of activated carbon fibers and precursors treated with ammonia. *Carbon* 2001;39(12):1809–20.
- [33] Mangun CL, DeBarr JA, Economy J. Adsorption of sulfur dioxide on ammonia-treated activated carbon fibers. *Carbon* 2001;39(11):1689–96.
- [34] Foster KL, Fuerman RG, Economy J, Larson SM, Rood MJ. Adsorption characteristics of trace volatile organic-compounds in gas streams onto activated carbon-fibers. *Chem Mater* 1992;4(5):1068–73.
- [35] Vidic RD, Tessmer CH, Uranowski LJ. Impact of surface properties of activated carbons on oxidative coupling of phenolic compounds. *Carbon* 1997;35(9):1349–59.
- [36] Feng W, Kwon S, Feng X, Borguet E, Vidic R. Adsorption of hydrogen sulfide onto activated carbon fibers: effect of pore structure and surface chemistry. *Environ Sci Technol* 2005;39(24):9744–9.
- [37] Li YH, Lee CW, Gullett BK. Importance of activated carbon's oxygen surface functional groups on elemental mercury adsorption. *Fuel* 2003;82(4):451–7.
- [38] Zhu ZH, Radovic LR, Lu GQ. Effects of acid treatments of carbon on N<sub>2</sub>O and NO reduction by carbon-supported copper catalysts. *Carbon* 2000;38(3):451–64.